Uncalibrated Euclidean 3-D Reconstruction Using an Active Vision System

Y. F. Li, *Senior Member, IEEE,* and R. S. Lu

***Abstract*—Uncalibrated reconstruction of a scene is desired in many practical applications of computer vision. However, using a single camera with unconstrained motion and unknown parameters, a true Euclidean three-dimensional (3-D) model of the scene cannot be reconstructed. In this paper, we present a method for true Euclidean 3-D reconstruction using an active vision system consisting of a pattern projector and a camera. When the intrinsic and extrinsic parameters of the camera are changed during the reconstruction, they can be self-calibrated and the real 3-D model of the scene can then be reconstructed. The parameters of the projector are precalibrated and are kept constant during the reconstruction process. This allows the configuration of the vision system to be varied during a reconstruction task, which increases its self-adaptability to the environment or scene structure in which it is to work.**

***Index Terms*—Homography, self-calibration, three-dimensional (3-D) reconstruction, uncalibrated reconstruction.**

I. Introduction

RECONSTRUCTION of the three-dimensional (3-D) model of a scene from images is important to many practical applications, including reverse engineering, object recognition, and synthesis of virtual environments. Passive vision, including stereovision, has been attempted for this purpose. In the past, this would require dedicated devices for calibrating the intrinsic and extrinsic parameters of the cameras. Due to the special calibration target needed, such a calibration is normally carried out offline before a task begins. In many practical applications, online calibration during the execution of a task is needed. Over the years, efforts have been made in the research to achieve efficient online calibrations. Maybank and Faugeras [1] suggested the calibration of a camera using image correspondences in a sequence of images from a moving camera. The kinds of constructions that could be achieved from a binocular stereo rig were further addressed in [2]. It was found that a unique *projective* representation of the scene up to an arbitrary projective transformation could be constructed, if five arbitrary correspondences were chosen, and an *affine* representation of the scene up to an arbitrary affine transformation could be constructed, if four arbitrary correspondences were adopted. Hartly [3] gave a practical algorithm for Euclidean reconstruction from several views with the same camera based on Levenberg–Marquardt minimization. A new approach based on stratification was introduced in [4], and various efforts have been made in the research in recent years [5].

In this context, much work has been conducted in Euclidean reconstruction up to a transformation. Pollefeys *et al.* [6] proposed a method to obtain a Euclidean reconstruction from images taken with an uncalibrated camera with variable focal lengths. This method is based on an assumption that although the focal length is varied, the principal point of the camera remains unchanged. This assumption limits the range of applications of this method. Similar assumptions were also made in the investigations in [7] and [8]. In practice, when the focal length is changed (e.g., by zooming), the principal point may vary as well. In the work by Heyden and Åström [9], they proved that it is possible to obtain Euclidean reconstruction up to a scale, using an uncalibrated camera with known aspect ratio and skew parameters of the camera. A special case of *a camera with a Euclidean image plane* was used for their study. A crucial step in the algorithm is the initialization, which will affect the convergence. How to obtain a suitable initialization was still an issue to solve [10]. Kahl [11] presented an approach to self-calibration and Euclidean reconstruction of a scene, assuming an affine model with zero skew for the camera. Other parameters, such as the intrinsic parameters, could be unknown or varied. The reconstruction, which needed a minimum of three images, was an approximation and was up to a scale. Pollefeys *et al.* gave the minimum number of images needed for achieving metric reconstruction, i.e., to restrict the projective ambiguity to a metric one according to the set of constraints available from each view [10].

The above reconstruction methods are based on passive vision systems. As a result, they suffer from the ambiguity of correspondences between the camera images, which is a difficult problem to solve, especially when free-form surfaces [12] are involved in the scene. To avoid the problem, active vision can be adopted. Structured light or pattern projection systems have been used for this purpose. To precisely reconstruct a 3-D shape with such a system, the active vision system, consisting of a projector and a camera, needs to be carefully calibrated [13], [14]. The traditional calibration procedure normally involves two separate stages: camera calibration and projector calibration. These individual calibrations are carried out offline, and they have to be repeated each time the setting is changed. As a result, the applications of active vision systems are limited, since the system

Manuscript received June 22, 2002; revised March 19, 2003. This paper was recommended for publication by Associate Editor Y. Liu and Editor S. Hutchinson upon evaluation of the reviewers' comments. This work was supported by a grant from the Research Grants Council of Hong Kong, under Project CityU1049/00E.

Y. F. Li is with the Department of Manufacturing Engineering and Engineering Management, City University of Hong, Kowloon, Hong Kong (e-mail: meyfli@cityu.edu.hk).

R. S. Lu was with the Department of Manufacturing Engineering and Engineering Management, City University of Hong, Kowloon, Hong Kong. He is now with the Mechanical Engineering Department, Imperial College London, London SW7 2BX, U.K.

Digital Object Identifier 10.1109/TRA.2003.820925

configuration and parameters must be kept unchanged during the entire measurement process. In some applications, such as seabed metric reconstruction with an underwater robot, when the size or distance of the scene changes, the configuration and parameters of the vision system need to be changed to optimize the measurement. In such applications, uncalibrated reconstruction is needed. In this regard, efforts have been made in recent research. Fofi *et al.* [15] studied the Euclidean reconstruction by means of an uncalibrated structured light system with a color-coded grid pattern. They modeled the pattern projector as a pseudocamera, and then the whole system as a two-camera system. Uncalibrated Euclidean reconstruction was performed with varying focus, zoom, and aperture of the camera. The parameters of the structured light sensor were computed according to the stratified algorithm [4], [5]. However, it was not clear how many of the parameters of the camera and projector could be self-determined in the uncalibrated reconstruction process. Further investigation is needed in uncalibrated Euclidean 3-D reconstruction, using an active vision system when the parameters of the camera and the configuration of the vision system are changed.

In this paper, we present a method of uncalibrated Euclidean 3-D reconstruction using an active vision system consisting of a light pattern projector and a camera. The pattern projector is assumed to be precalibrated offline, whereas both the intrinsic and extrinsic parameters of the camera can be changed or even totally unknown at the beginning of a reconstruction task. This allows uncalibrated reconstruction of the 3-D models of a scene and makes the vision system self-adaptable to the environment in which it is to work. This paper is organized as follows. In Section II, we introduce the notations and the basic principles related to projective geometry which will be used throughout the paper. Section III gives the projective model of our active vision system. The calibration method for the light pattern projector is described in Section IV. In Section V, the method for the uncalibrated Euclidean 3-D reconstruction is developed. Section VI gives the experimental results in the implementation. Section VII contains some conclusions drawn from the investigation.

II. Projective Geometry in 3-D Space

In this section, we will derive and prove some theorems related to projective geometry which will be used thereinafter. First, we will define the notations used in the paper.

$\Pi, \Pi_k \ldots$ represent the projective planes. The image plane of the charge-coupled device (CCD) camera is defined by Π, and the kth light stripe plane by Π_k.

$F_w, F_\Pi, F_{\Pi_k}, F_{2\Pi_k}, F_{3\Pi_k} \ldots$ represent the coordinate frames. The subscript "2" specifies a 2-D coordinate frame, and "3" defines a 3-D coordinate frame. We denote the known world coordinate frame by F_w, image coordinate system by F_Π, and the coordinate frame of the kth stripe light plane by F_{Π_k}. The notation F_{Π_k} usually represents both $F_{2\Pi_k}$ and $F_{3\Pi_k}$, when not given explicitly.

$M, \boldsymbol{M}, \tilde{\boldsymbol{M}}, m, \boldsymbol{m}, \tilde{\boldsymbol{m}}, \ldots$. An italic upper-case letter refers to a point in space, which may be on a line or a plane. The bold italic upper-case letter is used to denote the regular coordinates, e.g., $\boldsymbol{M} = (M_1, M_2, M_3)^{\mathrm{T}}$. The homogeneous or projective coordinates are denoted by adding a "$\sim$," e.g., $\tilde{\boldsymbol{M}} = (M_1, M_2, M_3, 1)^{\mathrm{T}}$. Similarly, an italic lower-case letter refers to a point in image plane or stripe light plane relative to the projective space. The bold one refers to its 2-D coordinates, e.g., $\boldsymbol{m} = (m_1, m_2)^{\mathrm{T}}$ and its homogeneous one $\tilde{\boldsymbol{m}} = (m_1, m_2, 1)^{\mathrm{T}}$. The reader is reminded that $\tilde{\boldsymbol{M}}$ and $k\tilde{\boldsymbol{M}}$, for any nonzero scalar k, denote the same point.

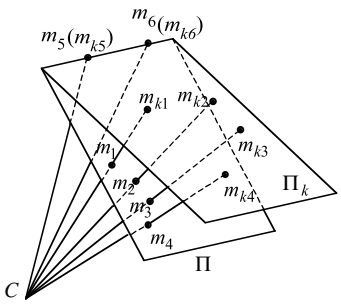

Fig. 1. Plane-to-plane homography.

A. Homography

In 3-D projective geometry, the term homography refers to the plane-to-plane transformation in the projective space [16], [17]. Given four or more distinct noncollinear points $\tilde{\boldsymbol{m}}_i$, where $i = 1, 2, \ldots, n$ for $n > 4$, on a plane Π, and another four or more distinct noncollinear points $\tilde{\boldsymbol{m}}_{ki}$ on the other plane Π_k, there is one and only one perspectivity under a projective center C, which carries the first point set, respectively, into the second. There exists a unique homography H, defined up to a scale, such that

$$\boldsymbol{H}_k \tilde{\boldsymbol{m}}_i = \lambda_i \tilde{\boldsymbol{m}}_{ki} \tag{1}$$

where λ_i's are unknown scalars, and

$$\boldsymbol{H}_k = \begin{bmatrix} h_{11} & h_{12} & h_{13} \\ h_{21} & h_{22} & h_{23} \\ h_{31} & h_{32} & h_{33} \end{bmatrix} \text{ is a } 3 \times 3 \text{ matrix.}$$

Definition 1: Under a projectivity $\boldsymbol{H}$ in projective space Ω, a point $X \in \Omega$ is said to be an invariant point if $\boldsymbol{H}(X) = X$; a line L is said to be an invariant line if $\boldsymbol{H}(L) = L$; a line L is said to be pointwise invariant if $\boldsymbol{H}(L) = L$ and $\forall X \in L : \boldsymbol{H}(X) = X$.

Lemma 1: A projectivity P relating two planes in a projective space Ω is perspective if and only if the common line of the two planes is pointwise invariant [18].

Fig. 1 explains the implication of this lemma, which can be seen as a natural extension of a similar theorem concerning the projectivity relating two lines on a plane.

Theorem 1: In projective space Ω, if two projective planes $\boldsymbol{\Pi}_1$ and $\boldsymbol{\Pi}_2$ have homographies $\boldsymbol{H}_1$ and $\boldsymbol{H}_2$ with respect to a common projective plane Π under a projective center C, then the two projective homographies will follow:

$$\boldsymbol{H}_2 \boldsymbol{H}_1^{-1} \boldsymbol{S} T_1 \tilde{\boldsymbol{P}} = \lambda \boldsymbol{S} T_2 \tilde{\boldsymbol{P}} \tag{3}$$

$$\boldsymbol{H}_2 \boldsymbol{H}_1^{-1} \boldsymbol{Q} R_1 \boldsymbol{n}_1 \times \boldsymbol{n}_2 = \lambda \boldsymbol{Q} R_2 \boldsymbol{n}_1 \times \boldsymbol{n}_2 \tag{4}$$

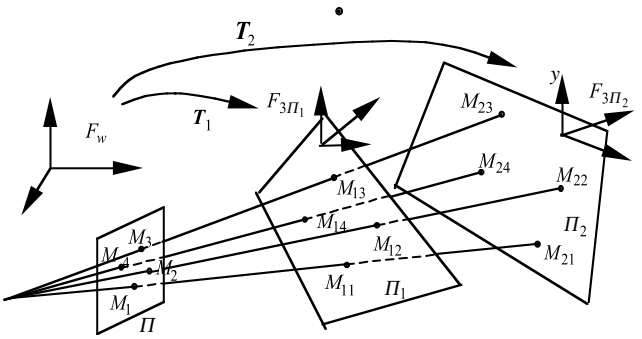

Fig. 2. Relations between the homographies of two planes in a projective space.

where λ is a scale factor. $\tilde{\boldsymbol{P}}_i$ is the homogeneous coordinates of a arbitrary point on the cross line between the light planes 1 and 2, with respect to a world coordinate system. $\boldsymbol{n}_1$ and $\boldsymbol{n}_2$ represent the normal vectors of the two projective planes, respectively. $\boldsymbol{T}_1$ and $\boldsymbol{T}_2$, and $\boldsymbol{R}_1$ and $\boldsymbol{R}_2$, are the two planes' transformations relative to the world coordinate system, respectively. They are related by

$$\boldsymbol{T}_i = \begin{bmatrix} \boldsymbol{R}_i & -\boldsymbol{R}_i\bar{\boldsymbol{M}}_i \\ \boldsymbol{0}^T & 1 \end{bmatrix}, \quad (i = 1, 2) \tag{5}$$

if defining the principal points of the local coordinates on the two planes as $\bar{\boldsymbol{M}}_i (i = 1, 2)$ relative to the world coordinate system. The other constant matrices are

$$\boldsymbol{S} = \begin{bmatrix} 1 & 0 & 0 & 0 \\ 0 & 1 & 0 & 0 \\ 0 & 0 & 0 & 1 \end{bmatrix}$$
$$\boldsymbol{Q} = \begin{bmatrix} 1 & 0 & 0 \\ 0 & 1 & 0 \\ 0 & 0 & 0 \end{bmatrix}. \tag{6}$$

Proof: As shown in Fig. 2, if there exist three projective planes Π, Π_1, and Π_2 in the projective space Ω under the projective center C, let the world coordinate system be F_w, the 3-D local coordinate system of plane Π_1 be $F_{3\Pi_1}$, and that of plane Π_2 be $F_{3\Pi_2}$. Then, according to (1), we have

$$\begin{cases} \boldsymbol{H}_1\tilde{\boldsymbol{m}}_i = k_{1i}\tilde{\boldsymbol{m}}_{1i} \\ \boldsymbol{H}_2\tilde{\boldsymbol{m}}_i = k_{2i}\tilde{\boldsymbol{m}}_{2i}. \end{cases} \tag{7}$$

A point $\tilde{\boldsymbol{m}}_{1i} = (m_{1i}, m_{1i}, 1)^T$ relative to $F_{3\Pi_1}$ is given by $(m_{1i}, m_{1i}, 0, 1)^T$. In the same way, $\tilde{\boldsymbol{m}}_{2i} = (m_{2i}, m_{2i}, 1)^T$ is represented as $(m_{2i}, m_{2i}, 0, 1)^T$ relative to frame $F_{3\Pi_2}$. Let $\tilde{\boldsymbol{M}}_{1i}$ and $\tilde{\boldsymbol{M}}_{2i}$ be these points in $F_{3\Pi_1}$ and $F_{3\Pi_2}$, respectively, and then we have

$$\begin{cases} \boldsymbol{H}_1\tilde{\boldsymbol{m}}_i = k_{1i}\boldsymbol{S}\tilde{\boldsymbol{M}}_{1i} \\ \boldsymbol{H}_2\tilde{\boldsymbol{m}}_i = k_{2i}\boldsymbol{S}\tilde{\boldsymbol{M}}_{2i}. \end{cases} \tag{8}$$

Assume an arbitrary point $\boldsymbol{P}_i$ on the intersection line between the two planes, Π_1 and Π_2, and we have

$$\begin{cases} \boldsymbol{H}_1\tilde{\boldsymbol{m}}_i = k_{1i}\boldsymbol{S}T_1\tilde{\boldsymbol{P}}_i \\ \boldsymbol{H}_2\tilde{\boldsymbol{m}}_i = k_{2i}\boldsymbol{S}T_2\tilde{\boldsymbol{P}}_i. \end{cases}$$

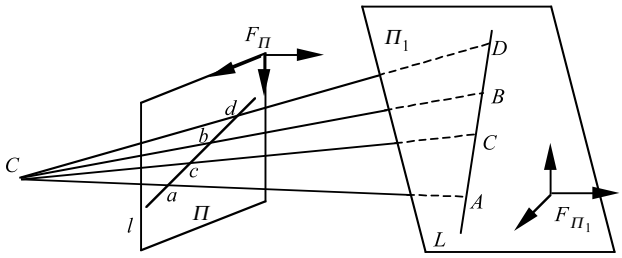

Fig. 3. Cross ratio.

Integrating the above formula yields

$$\boldsymbol{H}_2\boldsymbol{H}_1^{-1}\boldsymbol{S}T_1\tilde{\boldsymbol{P}}_i = \lambda_i\boldsymbol{S}T_2\tilde{\boldsymbol{P}}_i. \tag{9}$$

Expanding the above equation, we obtain

$$\boldsymbol{H}_2\boldsymbol{H}_1^{-1}\boldsymbol{Q}R_1\boldsymbol{n}_1 \times \boldsymbol{n}_2 = \lambda_i\boldsymbol{Q}R_2\boldsymbol{n}_1 \times \boldsymbol{n}_2. \tag{10}$$

From (9), it is seen that the scale factor λ_i is unique. That is to say, for all points on the common line of the two planes, the factors λ_i are equal. □

B. Cross Ratio

Assume four collinear points on the line L of the plane Π_1 in 3-D space, as illustrated in Fig. 3. Based on the properties of projective geometry, the four points' correspondences projected on the projective plane Π (such as a CCD camera-image plane) under projective center C are collinear on the corresponding line l of the line L. Thus, we have the following theorem.

Theorem 2: If four collinear points A, B, C, D are projected from a vertex C into four collinear points a, b, c, d, then [19]

$$(A, B; C, D) = (a, b; c, d) \tag{11}$$

where $(A, B; C, D)$ is called *cross ratio* and is given by

$$(A, B; C, D) = \frac{AC}{BC} \Big/ \frac{AD}{BD} \tag{12}$$

This theorem implies an important property of projective geometry: cross ratio is invariant under projection. In (12), none of $A, B, C, D = \infty$. In case one of A, B, C, or $D = \infty$, we set $(A, B; C, D) = (BD/BC)$ if A $= \infty, (BD/BC)$ if $B = \infty, (BD/AD)$ if $C = \infty$, and (AC/BC) if $D = \infty$ [20]. The cross ratio of any four points on a line is independent of the coordinate system established for the line. In particular, if points A, B, C, D are four points of the line L, with parameters $\theta_A, \theta_B, \theta_C, \theta_D$, then

$$(A, B; C, D) = \frac{\theta_A - \theta_C}{\theta_B - \theta_C} \Big/ \frac{\theta_A - \theta_D}{\theta_B - \theta_D} \tag{13}$$

III. Active Visual Sensing Using Pattern Projections

The structure of our vision system is illustrated in Fig. 4. A projector is used to illuminate the scene to be measured with a pattern of light which consists of n plane stripes here. Each of the stripes intersecting with the scene produces a deformed curve on its light plane in 3-D space F_w. The pattern of the

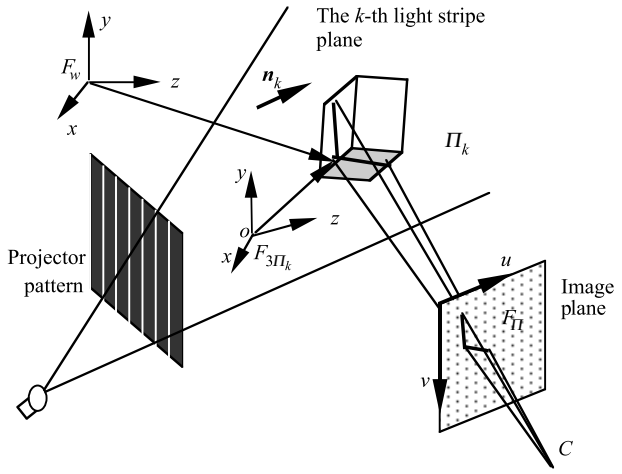

Fig. 4. Structure of the active vision system.

curves is then detected using a camera, and the scene can be reconstructed in the image processing.

Here, we will model the system via homographic transformation of each light stripe plane relative to the camera. Assume a world coordinate system F_w with three coordinate axes (x, y, z). For each of the stripe planes, if we know a point on it, then we can define a coordinate frame on it. A simple way is to translate the origin of the world coordinate system to this known point on the stripe light plane, and then rotate it around a vector perpendicular to its z axis and the normal vector of the stripe light plane until its xy plane is aligned with the stripe light plane.

Suppose the normal vector of the kth stripe light plane Π_k is $\boldsymbol{n}_k = (n_{k1}, n_{k2}, n_{k3})^T$ in the frame F_w. The angle θ between $\boldsymbol{n}_k$ and the z axis of the frame $F_w, \boldsymbol{z} = (0, 0, 1)^T$, is simply the inner product of the two vectors

$$\theta = \cos^{-1}(\boldsymbol{n}^T \boldsymbol{z}) = \cos^{-1}(n_{k3}). \tag{14}$$

The unit vector, $\boldsymbol{r} = (r_1, r_2, r_3)$, perpendicular to both the z axis of the frame F_w and the normal vector $\boldsymbol{n}_k$, is

$$\boldsymbol{r} = (\boldsymbol{n}_k \times \boldsymbol{z})/\|\boldsymbol{n}_k \times \boldsymbol{z}\|. \tag{15}$$

Then the rotation matrix can be given by *Rodrigues' formula*

$$\boldsymbol{R} = \cos\theta \cdot \boldsymbol{I} + (1 - \cos\theta)\boldsymbol{r}r^T + \sin\theta \cdot \boldsymbol{r}_\wedge \tag{16}$$

where $\boldsymbol{r}_\wedge$ is the skew-symmetric matrix, i.e.,

$$\boldsymbol{r}_\wedge = \begin{bmatrix} 0 & -r_3 & r_2 \\ r_3 & 0 & -r_1 \\ -r_2 & r_1 & 0 \end{bmatrix}. \tag{17}$$

If $\boldsymbol{n}_k$ and $\boldsymbol{r}$ are parallel, then $\theta = 0$, and $\boldsymbol{R} = \boldsymbol{I}$.

Assuming the origin of the frame $F_{3\Pi_k}$ being $\bar{\boldsymbol{M}}_k = (\bar{M}_{k1}, \bar{M}_{k2}, \bar{M}_{k3})^{\mathrm{T}}$, the transformation between the frames F_w and $F_{3\Pi_k}$ can be represented by

$$\boldsymbol{T}_k = \begin{bmatrix} \boldsymbol{R} & -\boldsymbol{R}\bar{\boldsymbol{M}}_k \\ \boldsymbol{0}^T & 1 \end{bmatrix}. \tag{18}$$

If an arbitrary point on the stripe light plane is defined as $\boldsymbol{M}_{ki} = (M_{k1}, M_{k2}, M_{k3})^{\mathrm{T}}$, its homogeneous coordinates are $\tilde{\boldsymbol{M}}_{ki} = (M_{k1}, M_{k2}, M_{k3}, 1)^{\mathrm{T}}$. Then matrix $\boldsymbol{T}_k$ would transform the world point $\tilde{\boldsymbol{M}}_{ki}$ in frame F_w into the following in frame $F_{3\Pi_k}$:

$$\boldsymbol{T}_k \tilde{\boldsymbol{M}}_{ki} = (m_{k1}, m_{k2}, 0, 1)^{\mathrm{T}}.$$

Thus, the coordinate relation between the world coordinate system F_w and the coordinate system of stripe light plane $F_{2\Pi_k}$ follows:

$$\boldsymbol{T}_k \tilde{\boldsymbol{M}}_{ki} = \boldsymbol{S}^T \tilde{\boldsymbol{m}}_{ki} \tag{19}$$

where $\tilde{\boldsymbol{m}}_{ki} = (m_{k1}, m_{k2}, 1)$ is the corresponding homogenous coordinates of $\boldsymbol{M}_{ki}$ in frame $F_{2\Pi_k}$; $\boldsymbol{S}$ is defined in (6). The equation of the stripe light plane in frame F_w is given by

$$\boldsymbol{n}_k^T(\boldsymbol{M}_k - \bar{\boldsymbol{M}}_k) = 0. \tag{20}$$

As for the camera, we will model it as a projective one using a pinhole model. As shown in Fig. 4, the optical center of the camera is used as the projective center C. The coordinate system on the image plane is defined to have its origin at the upper-left corner of the image plane, as shown in Fig. 4. We denote this coordinate frame as F_Π. According to (2), given $\boldsymbol{m}_{ki} \in F_{2\Pi_k}, \forall \boldsymbol{m}_i \in F_\Pi$, the relation between them satisfies

$$\boldsymbol{H}_k \tilde{\boldsymbol{m}}_i = \lambda_i \tilde{\boldsymbol{m}}_{ki}.$$

Substituting this equation into (19), we obtain

$$\lambda_i \boldsymbol{T}_k \tilde{\boldsymbol{M}}_{ki} = \boldsymbol{S}^T \boldsymbol{H}_k \tilde{\boldsymbol{m}}_i. \tag{21}$$

That is

$$\tilde{\boldsymbol{M}}_{ki} = \rho \boldsymbol{T}_k^{-1} \boldsymbol{S}^T \boldsymbol{H}_k \tilde{\boldsymbol{m}}_i. \tag{22}$$

The formula can be expanded to

$$\boldsymbol{M}_{ki} = \bar{\boldsymbol{M}}_{ki} + \frac{\boldsymbol{R}_k^T \boldsymbol{Q} H_k \tilde{\boldsymbol{m}}_i}{\boldsymbol{e}^T \boldsymbol{H}_k \tilde{\boldsymbol{m}}_i} \tag{23}$$

where $\boldsymbol{e} = [0 \quad 0 \quad 1]^T$. Equations (22) and (23) are the model equations of our vision system using the pattern projection.

IV. Precalibration of the Projector

In our work, the projector is precalibrated at an offline stage. Although this requirement seems to be a limitation of the approach, from the engineering point of view, this is acceptable, as a projector can be expected to be accurately calibrated at the manufacturer or laboratory floor. In many practical applications, it is the camera and its relative pose that need to be online adjusted. Assuming a calibrated projector allows more camera parameters to be changed and calibrated online [13], [14]. Here, rather than using affine transform [11], the calibration follows the plane-based formulation using homography to take advantage of the stripe planes in the pattern projection. This also overcomes the potential problem due to the nonpoint nature of the light source if the projector is modeled as a pseudocamera, as adopted by others [15]. Here, our method to calibrate the stripe light plane is based on cross-ratio invariant and *point-to-point* calibration [16], [21]. To improve the calibration accuracy, we

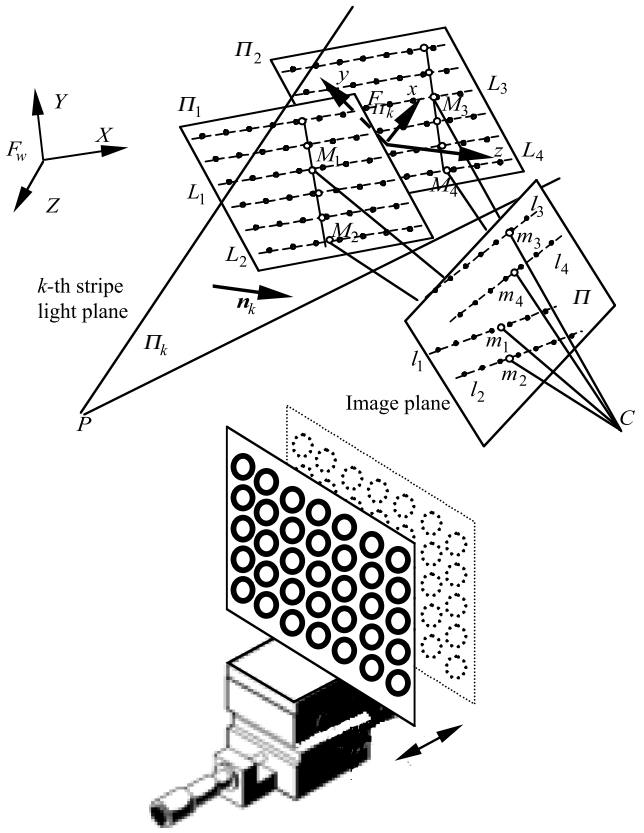

Fig. 5. Calibration of the light stripe projector.

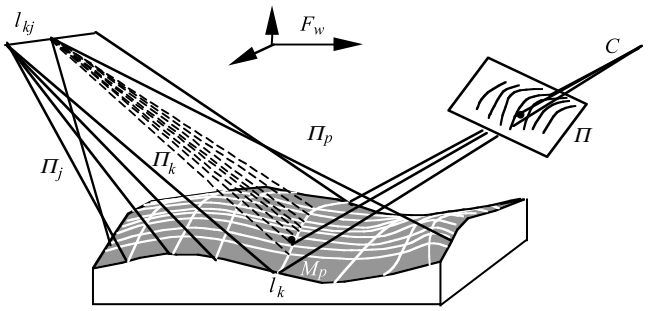

Fig. 6. Uncalibrated reconstruction.

used a pattern plane with many circles on it as a calibration target to produce a number of known points in the world coordinate system, instead of four known noncoplanar sets of three collinear world points, as used by Huynh *et al.* [16].

Define

$$\boldsymbol{T}_{wk} = \boldsymbol{T}_k^{-1}\boldsymbol{S}^T\boldsymbol{H}_k \tag{24}$$

as the kth image to world (2-D–3-D) transformation between a 3-D point on the kth stripe light plane, relative to frame F_w and its correspondence on the image plane of the camera. Here, $\boldsymbol{T}_{wk}$ is a 4×3 matrix with 12 unknown parameters, but with only 11 independent. For each stripe light plane and its $\boldsymbol{T}_{wk}$, a point on the plane and its correspondence on the image plane will give three independent equations based on (23). Therefore, to compute the transformation $\boldsymbol{T}_{wk}$, at least four points' 3-D coordinates on the plane and their correspondences on the image plane need to be known.

Here, a precision 1-D translation stage is used to move the calibration target to different positions, as shown in Fig. 5. When the calibration pattern plane is moved to a different position, the stripe light plane will intersect with line L_i on the pattern plane and produce a number of points M_i. The correspondence of the points, m_i, will appear on the image plane. As mentioned above, any four or more points in general positions define a stripe light plane, and their corresponding image projections define a unique homography $\boldsymbol{H}_k$. To obtain $\boldsymbol{H}_k$, the calibration pattern plane will be placed at two positions, at least. Three positions are normally sufficient to achieve a reasonably high calibration accuracy. The calibration procedure is given as follows.

Step 1) Based on (12) and (13), compute the 3-D coordinates of the points, $M_i(i \geq 4)$, on the kth stripe light plane relative to the world coordinate frame F_w. Any point coordinates on a four-point collinear line can be obtained if the coordinates of the other three points are known. As shown in Fig. 6, more than four known points can be collinear on both the calibration pattern plane and the image plane. To improve the computing accuracy of a point M_i, besides the unknown point M_i, we should arbitrarily select three other known points on the collinear line on the pattern plane and their correspondence on the image plane to compute the cross ratio and the point M_i's coordinates relative to the world coordinate frame. Then use the mean value of these results as the estimate of the point M_i's coordinates.

Step 2) Compute the unit normal vector $\boldsymbol{n}_k$ and correct the point M_i's coordinates. As shown in Fig. 6, if the equation of the kth stripe light plane relative to frame F_w were known, we could easily obtain its unit normal vector $\boldsymbol{n}_k$. Unfortunately, this is not the case in practice. Nevertheless, we can reconstruct the equation of the stripe plane and its unit normal vector from the known points M_i. Under the constraint condition of a stripe light plane, all the points M_i on the kth stripe light plane should be coplanar. In practice, due to projective and computational errors, the points M_i may not all be exactly coplanar. Thus, we use the least square method to reconstruct the light plane and its unit normal vectors. Then we project all of the points M_i onto the least square plane in Euclidean space F_w, and use the coordinates of these projective points as the estimations for them.

Step 3) Establish the stripe light plane coordinate system F_{Π_k} ($F_{2\Pi_k}$ and $F_{3\Pi_k}$) and compute the world-to-stripe light plane transformation $\boldsymbol{T}_k$. Since the homography exists regardless of the choice of the 2-D coordinate frames in the projective planes, $F_{2\Pi_k}$ and $F_{3\Pi_k}$ can be arbitrarily defined. Without loss of generality, the centroid $\bar{\boldsymbol{M}}_k$ of the computed world points $M_i(i \geq 4)$ is used as the origin of the coordinate frame. The frames $F_{2\Pi_k}$ and $F_{3\Pi_k}$ are set up by translating the origin of the frame F_w to the centroid $\bar{\boldsymbol{M}}_k$, and then rotating around the unit vector $\boldsymbol{r}$ perpendicular to both the z axis of the

frame F_w and the unit normal vector of the stripe light plane $\boldsymbol{n}_k$ to align the $x-y$ coordinates plane of the frame F_w with the stripe light plane. Using (14)–(19), we can compute the world-to-stripe light plane transformation $\boldsymbol{T}_k$.

Step 4) Go to step 1 and compute the other stripe light plane transformations until all of them are obtained.

V. Uncalibrated Reconstruction

After the parameters of the projector (i.e., the unit normal vector $\boldsymbol{n}_k$ of stripe light plane, the origin $\bar{\boldsymbol{M}}_k$ of the frames $F_{2\Pi_k}$ and $F_{3\Pi_k}$, and the world-to-stripe light plane transformation $\boldsymbol{T}_k$) are obtained, we can use the active vision system to carry out uncalibrated reconstructions of a scene surface, even though the parameters of the camera are unknown or varying. The crucial problem in the uncalibrated reconstruction is how to self-recover these unknown parameters. That is, how to self-calibrate the unknown homographic matrix $\boldsymbol{H}_k$ between the stripe light planes Π_k and camera image plane Π.

A. Basic Principle

As shown in Fig. 6, when the kth stripe light plane Π_k intersects with the scene, a curve l_k on the stripe light plane Π_k will be illuminated. If an arbitrary point on the curve is identified as M_p and, simultaneously, the point is on a known plane Π_p in the world frame F_w, then the point satisfies the equation of plane Π_p

$$\left(\boldsymbol{n}_p^T, -\boldsymbol{n}_p^T\bar{\boldsymbol{M}}_p\right)\tilde{\boldsymbol{M}}_p = 0 \tag{26}$$

where $\boldsymbol{n}_p$ is the plane's normal vector and the $\bar{\boldsymbol{M}}_p$ is a known point on the plane. As point M_p is also on the stripe light plane, substituting (22) into the plane equation above, we obtain

$$\left(\boldsymbol{n}_p^T, -\boldsymbol{n}_p^T\bar{\boldsymbol{M}}_p\right)\boldsymbol{T}_k^{-1}\boldsymbol{S}^T\boldsymbol{H}_k\tilde{\boldsymbol{m}}_{kp} = 0 \tag{27}$$

where $\tilde{\boldsymbol{m}}_{kp}$ is the projective point on the camera image plane of point M_p. In (27), the unknown argument is the homographic matrix of the stripe light plane $\boldsymbol{H}_k$, which has eight independent unknown elements. If we have eight or more general points on the curve lying on eight or more known planes, we can obtain eight independent equations, based on (27). Then the unknown homographic matrix $\boldsymbol{H}_k$ can be solved. According to (22) or (23), the scene can then be reconstructed in Euclidean space. The crucial issue is how to obtain the eight or more known planes. As illustrated in Fig. 6, if adding much more than eight stripe light planes $\Pi_p(p=1,2,\ldots,p_{\max}>8)$ perpendicular to or intersecting with the stripe light plane $\Pi_k(k=1,2,\ldots)$, this problem can be solved. The parameters of these stripe planes can be obtained at the precalibration stage for the projector.

B. Algorithm

For the matrix, shown at the bottom of the page, assuming two points $\boldsymbol{M}_p$ and $\boldsymbol{M}_k$, the third row of the vector $\boldsymbol{P}$ is nonzero. Define

$$\begin{cases} \boldsymbol{P} = [k_1 \quad k_2 \quad k_3]^T \\ \tilde{\boldsymbol{m}'} = \left[\frac{k_1}{k_3} \quad \frac{k_2}{k_3} \quad 1\right]^T = [u' \quad v' \quad 1]^T \\ \boldsymbol{m} = \tilde{\boldsymbol{m}}_{kp} = [u \quad v \quad 1]^T. \end{cases} \tag{30}$$

Then (27) can be simplified to

$$\boldsymbol{m}'^T\boldsymbol{H}m = 0.$$

The above equation can be expanded to

$$\begin{bmatrix} u_1'u_1 & u_1'v_1 & u_1' & v_1'u_1 & v_1'v_1 & v_1' & u_1 & v_1 & 1 \\ \vdots & \vdots & \vdots & \vdots & \vdots & \vdots & \vdots & \vdots & \vdots \\ u_n'u_n & u_n'v_n & u_n' & v_n'u_n & v_n'v_n & v_n' & u_n & v_n & 1 \end{bmatrix}\boldsymbol{h} = 0 \tag{31}$$

where $\boldsymbol{h} = (h_{11}, h_{12}, h_{13}, h_{21}, h_{22}, h_{23}, h_{31}, h_{32}, h_{33})^T$, and then simplified as

$$\boldsymbol{A}h = 0. \tag{32}$$

According to (2), the homography between the stripe light plane and the camera image plane is a unique one up to a scale factor. To solve for the homography, the following approach is taken.

Equation (31) can be expanded to

$$\begin{aligned}(u'h_{11} + v'h_{21} + h_{31})u + (u'h_{12} + v'h_{22} + h_{32})v \\ + (u'h_{13} + v'h_{23} + h_{33}) = 0\end{aligned} \tag{33}$$

and then further simplified as

$$a\cdot u + b\cdot v + c = 0 \tag{34}$$

where

$$\begin{cases} a = u'h_{11} + v'h_{21} + h_{31} \\ b = u'h_{12} + v'h_{22} + h_{32} \\ c = u'h_{13} + v'h_{23} + h_{33}. \end{cases} \tag{35}$$

Assume that only the image coordinates u and v will change, whereas a, b, and c are kept constant. Using more than two sets

$$\boldsymbol{T}^{-1} = \begin{bmatrix} \boldsymbol{R} & -\boldsymbol{R}\bar{\boldsymbol{M}} \\ \boldsymbol{0}^T & 1 \end{bmatrix}^{-1} = \begin{bmatrix} \boldsymbol{R}^T & \bar{\boldsymbol{M}} \\ 0 & 1 \end{bmatrix} \tag{28}$$

$$\begin{aligned}\boldsymbol{K} &= \left(\boldsymbol{n}_p^T, -\boldsymbol{n}_p^T\bar{\boldsymbol{M}}_p\right)\boldsymbol{T}_k^{-1}\boldsymbol{S}^T \\ &= \begin{bmatrix} n_{p1}r_{11} + n_{p2}r_{12} + n_{p3}r_{13} \\ n_{p1}r_{21} + n_{p2}r_{22} + n_{p3}r_{23} \\ n_{p1}(M_{p1} - M_{k1}) + n_p(M_{p2} - M_{k2}) + n_p(M_{p3} - M_{k3}) \end{bmatrix}\end{aligned} \tag{29}$$

TABLE I
HOMOGRAPHIC RELATIONS BETWEEN STRIPE LIGHT PLANES

Projection center $\boldsymbol{C}$	(-4.071, -22.262, 212.802)		
$\overline{\boldsymbol{M}}_1$	$\overline{\boldsymbol{M}}_2$	$\overline{\boldsymbol{M}}_3$	$\overline{\boldsymbol{M}}_4$
(0.467, -10.000, 30.000)	(29.029, -10.000, 30.000)	(57.760, -10.000, 30.000)	(86.809, -10.000, 30.000)
$\boldsymbol{n}_1$	$\boldsymbol{n}_2$	$\boldsymbol{n}_3$	$\boldsymbol{n}_4$
(2.162, 51.783, -205.011)	(2.162, 51.783, -205.011)	(2.162, 51.783, -205.011)	(2.162, 51.783, -205.011)
$\boldsymbol{T}_1$	$\boldsymbol{T}_2$	$\boldsymbol{T}_3$	$\boldsymbol{T}_4$
- 0.123 0.011 -0.992 29.935 0.011 1.000 0.000 29.935 0.992 -0.009 -0.123 29.935 0 0 0 1	-0.081 0.008 -0.997 32.341 0.008 1.000 0.007 32.341 0.997 -0.007 -0.081 32.341 0 0 0 1	-0.038 0.005 -0.999 32.221 0.005 1.000 0.005 32.221 0.999 -0.005 -0.038 32.221 0 0 0 1	0.006 0.002 -1.000 29.491 0.002 1.000 0.002 29.491 1.000 -0.002 0.006 29.491 0 0 0 1
$\boldsymbol{H}_{12}$	$\boldsymbol{H}_{13}$	$\boldsymbol{H}_{14}$	Evaluated homography $\boldsymbol{H}'_{14}$
2.857 -0.030 270.300 0.030 2.472 15.936 -0.002 0.000 1	7.338 -0.111 917.895 0.117 6.011 56.741 -0.007 0.000 1	33.247 -0.627 4660.856 0.666 26.461 301.195 -0.038 0.002 1	33.247 -0.627 4660.856 0.666 26.461 301.195 -0.038 0.002 1
Estimation error	$\left\|\boldsymbol{H}'_{14}\right\|^2 - \left\|\boldsymbol{H}_{14}\right\|^2 = -1.922\times 10^{-7}$		

of the image coordinates (u, v), we can first solve the ratios of the variables a, b, and c, defined as

$$\begin{cases} \rho_1 = a/c \\ \rho_2 = b/c. \end{cases} \tag{36}$$

As shown in Fig. 6, when the vision system takes more than two images of an object from different viewpoints, all the points illuminated on the scene by the intersection line of the two stripe planes Π_p and Π_k satisfy the equation of the stripe light plane Π_p. The three variables, a, b, and c, are kept constant. These points' correspondences on the CCD image plane will be different. With six stripe light planes Π_p, from (36), we have the matrix

$$\begin{bmatrix} \rho_{11}u'_{11} & \rho_{11}v'_{11} & \rho_{11} & -\rho_{21} & -\rho_{21}v'_{11} \\ \vdots & \vdots & \vdots & \vdots & \vdots \\ \rho_{1p}u'_{pn} & \rho_{1p}v'_{pn} & \rho_{1p} & -\rho_{2p} & -\rho_{2p}v'_{pn} \end{bmatrix} \times \begin{bmatrix} h_{12} \\ h_{22} \\ h_{32} \\ h_{21} \\ h_{31} \end{bmatrix} = \begin{bmatrix} \rho_{21} \\ \vdots \\ \rho_{2n} \end{bmatrix}. \tag{37}$$

We can obtain the first two columns' elements of the homography $\boldsymbol{H}$ if defining $h_{11} = 1$. Using the following equation, the last column's elements can be obtained:

$$(\rho_1 - \rho_2)c = a - b. \tag{38}$$

We then normalize the homography by defining the homographic matrix's lower-right entry $h_{33} = 1$.

The accuracy achievable by the above method would be limited, as the algorithm is sensitive to the noise of the scene image and that of the vision system. This is due to the iterative nature of the algorithm, as can be seen from (33)–(38). To improve on the accuracy, a nonlinear optimization algorithm can be employed. Based on (27), we use the following objective function for the optimization:

$$F_{\min}(\boldsymbol{H}_k) = \sum_{p=1}^{N_p}\sum_{i}^{N_i} \left[\left(\boldsymbol{n}_p^T, -\boldsymbol{n}_p^T\bar{\boldsymbol{M}}_p\right)\boldsymbol{T}_k^{-1}\boldsymbol{S}^T\boldsymbol{H}_k\tilde{\boldsymbol{m}}_i\right]^2 \tag{39}$$

where p denotes the index to the horizontal stripe planes, and i is the index to the image point along the intersection line between the horizontal stripe planes and the kth vertical stripe light plane. The objective function can be optimized using the Levenberg–Marguardt algorithm. The remaining problem in the nonlinear optimization is how to determine the initial value of the homography $\boldsymbol{H}_k$. As described in the projector calibration in Section IV, we can obtain the homographies between the projector stripe light planes and the camera image plane. Here, we call the homographies the normal ones. In uncalibrated reconstruction, the homographies do not change significantly after the parameters of the camera are adjusted. We can thus use the normal homographies in the initialization of the optimization. In cases when the normal homographies are unknown or they changed significantly after the camera's parameters are adjusted, the algorithm given via (37) and (38) can be used to obtain the initialization for the optimization.

C. Discussion

In recovering the homographies, if the normal vector $\boldsymbol{n}_k$, the origin $\bar{\boldsymbol{M}}_k$ and the transformation $\boldsymbol{T}_k$ are obtained in the offline calibration and remain unchanged or are known during the reconstruction, we do not need to obtain all the light stripe planes' transformations relative to the camera. Instead, only the homographic relations between any two or more stripe light planes relative to the camera image plane will be needed. Those of the other light stripe planes relative to the camera image plane can

be obtained by *Theorem 1*. This makes the uncalibrated reconstruction more feasible and flexible.

Now rewrite (3) as

$$\boldsymbol{H}_k\boldsymbol{H}_j^{-1}\boldsymbol{S}T_j\tilde{\boldsymbol{P}}_i = \lambda_j\boldsymbol{S}T_k\tilde{\boldsymbol{P}}_i. \tag{40}$$

If the homography $\boldsymbol{H}_j, \boldsymbol{T}_j, \boldsymbol{T}_k$ and point $\tilde{\boldsymbol{P}}_i$ are known, the above equation will have nine independent unknowns, including the factor λ. If we select two points on an intersection line l_{kj} between two stripe planes Π_j and Π_k, (31) will provide five independent equations. Thus, during the online calibration, only two arbitrary light stripe planes' homographies relative to the camera need to be computed. The other homographies can be derived from (31).

In a case study as shown in Table I, we arbitrarily selected four light stripe planes, $\boldsymbol{n}_i(i = 1, 2, 3, 4)$, to simulate their homographic relations. Define the projective center as $\boldsymbol{C}$ and the plane $\boldsymbol{n}_1$ as the camera image plane. We can compute the homographies of the other three stripes planes with respect to plane $\boldsymbol{n}_1$. Assume known homographies $\boldsymbol{H}_{12}, \boldsymbol{H}_{13}$. Then based on (31), we can obtain the homography $\boldsymbol{H}_{14}$. The estimated value $\boldsymbol{H}_{14}^{'}$ and the estimation error are also given in Table I. The above result was obtained in the absence of noise. In practice, however, the offline calibration results for the projector are subject to errors. If we use only two arbitrary planes' homographies to derive the other planes' homographies, the accuracy achievable will be limited. In such a case, the knowledge of more than two known stripe planes will be desired to obtain the other stripe planes' homographies.

D. Implementation Procedures

The implementation of the uncalibrated 3-D Euclidean reconstruction with unknown intrinsic and extrinsic parameters in the camera consists of two steps: the precision calibration of the projector and reconstruction with an uncalibrated camera. The procedure for the projector calibration is given in Section IV. After the parameters of the stripe light projector have been obtained, the vision system can be used for uncalibrated Euclidean reconstruction without knowing the camera parameters. The procedure of the uncalibrated Euclidean reconstruction consists of the following steps.

- Step 1) Based on the scene properties, adjust the projector's position and orientation to illuminate the scene properly. The projector's transformation with respect to the world frame is assumed to be known. Then adjust the camera's parameters, including its orientation, optical length, and zoom, as needed to enable the visual sensor to capture the illuminated scene fully. Then acquire the scene image.
- Step 2) According to the scene image, use the algorithm developed in Section V-B to compute the homographies of the stripe light planes with respect to the camera image plane.
- Step 3) After the homography $\boldsymbol{H}_k$ between the kth stripe light plane and the image plane of camera is obtained, use (23) to reconstruct the scene.

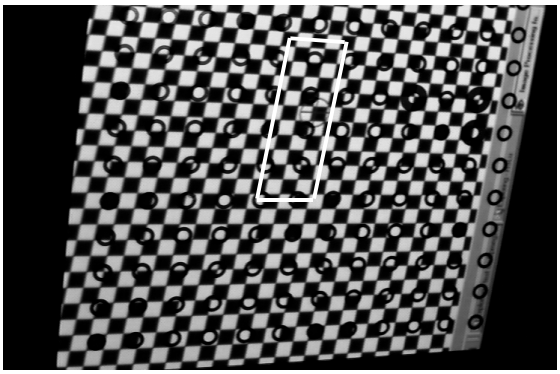

Fig. 7. Projection pattern.

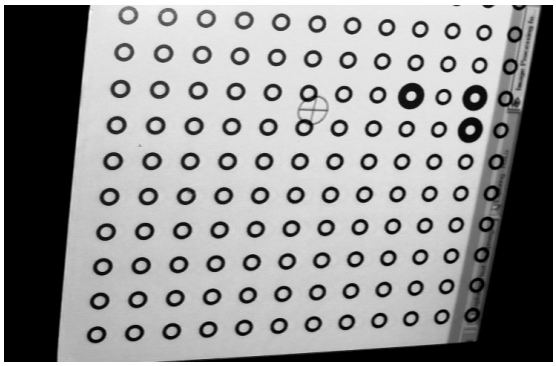

Fig. 8. Calibration target.

TABLE II
VERTICAL PLANE FITTING ERRORS (UNIT: mm)

	Vertical plane fitting errors			
	max	min	mean	sigma
1	0.0255	0.0693	0.0014	0.0198
2	0.0386	0.0981	0.0013	0.0249
3	0.0159	0.0399	0.0010	0.0109
4	0.0372	0.0933	0.0009	0.0264

TABLE III
VERTICAL PLANE HOMOGRAPHIC ERRORS (UNIT: mm)

	Vertical plane homographic errors			
	max	min	mean	sigma
1	0.2106	0.0129	0.0944	0.0458
2	0.2371	0.0145	0.1025	0.0501
3	0.1960	0.0070	0.0834	0.0425
4	0.2479	0.0173	0.0962	0.0483

VI. EXPERIMENTS

The active vision system used in our experiment consists of an LCD pattern projector and a CCD camera. To obtain the horizontal and vertical stripe light planes, we projected the pattern of white and black square grids, as shown in Fig. 7. To maximize the angles between the two adjacent stripe planes, the stripe planes were chosen to evenly span the entire range of the projector's field of view (FOV). The calibration object is a metal

TABLE IV
SELF-CALIBRATION RESULTS OF STRIPE LIGHT PLANES' HOMOGRAPHIES

Planes	H_1			H_2			H_3			H_4		
Standard H_S	0.6107	-195.9155	0.0827	0.6210	0.0850	-212.4794	0.6338	0.0876	-229.9556	0.6456	0.0901	-247.8107
	-0.0945	0.5022	-93.3482	-0.0968	0.5110	-92.6657	-0.1003	0.5194	-91.5238	-0.1031	0.5290	-90.7105
	0.0005	0.0000	1.0000	0.0005	0.0000	1.0000	0.0006	0.0000	1.0000	0.0006	0.0000	1.0000
Recovered H_R	0.6592	0.0764	-195.8976	0.6754	0.0704	-212.4642	0.6259	0.0859	-229.9428	0.6433	0.0852	-247.7863
	-0.1048	0.5029	-93.08630	-0.1086	0.5134	-92.3818	-0.0991	0.5195	-91.3269	-0.1031	0.5292	-90.3592
	0.0006	-0.0000	1.0000	0.0006	-0.0000	1.0000	0.0006	0.0000	1.0000	0.0006	-0.0000	1.0000
Error $H_R - H_S$	0.0484	-0.0063	0.0179	0.0544	-0.0145	0.0151	-0.0078	-0.0016	0.0128	-0.0023	-0.0049	0.0244
	-0.0103	0.0006	0.2619	-0.0117	0.0024	0.2840	0.0011	0.0001	0.1969	-0.0000	0.0003	0.3513
	0.0001	-0.0000	0.0000	0.0001	-0.0000	0.0000	-0.0000	-0.0000	0.0000	-0.0000	-0.0000	0.0000
Error $\|H_R - H_S\|^2$	0.267			0.290			0.197			0.352		

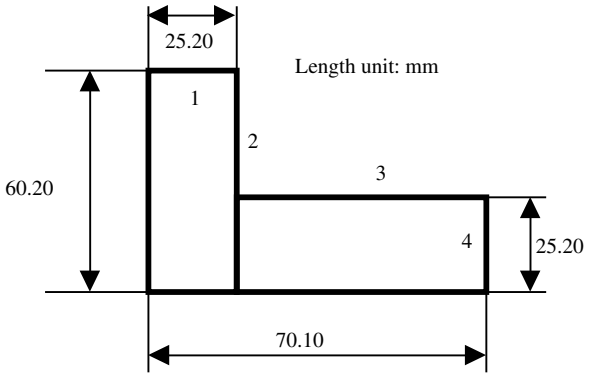

Fig. 9. Workpiece dimensions.

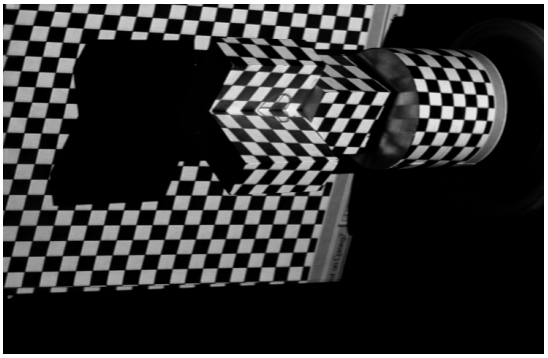

Fig. 10. Image of the workpiece.

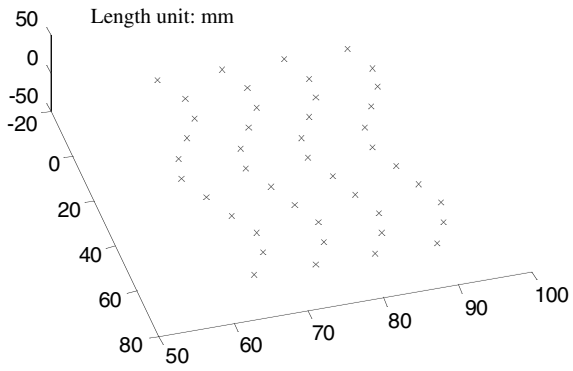

Fig. 11. Reconstructed 3-D points.

TABLE V
DISTANCE ERRORS IN UNCALIBRATION RECONSTRUCTION (UNIT: mm)

	plane1 to plane3	plane2 to plane 4
Standard distance	35.00	49.90
Recovered distance	34.84	44.95
Distance error	-0.06	0.05

plate with an array of circular rings, as shown in Fig. 8. This calibration object is for use in precalibrating the normal vectors of the stripe light planes only. Least-square fitting method was employed in obtaining the equations of the vectors in the world frame. The fitting errors, defined as the distance of the corresponding spatial points from the fitted stripe planes, are given in Table II. Here, we listed only the results of the 11×4 stripe light planes in the rectangular area in Fig. 7. The homographic errors, defined as the distance of the back-projected spatial points of the corresponding points on the image from their corresponding stripe light planes, are given in Table III. As a comparison, we used the image points and the corresponding points in the world frame to compute the vertical stripe planes' homographies relative to the camera image plane. The results are given in the second row of Table IV. Then we used the points on the image plane and the calibrated normal vectors of the stripe light planes to conduct the uncalibrated reconstruction of the vertical stripe light planes' homographies, with the results given in the third row of Table IV. In this implementation, the result was obtained using the nonlinear optimization algorithm given in Section V-B. The homographic errors relative to their standard value are listed in the fourth and fifth rows of Table IV. The results in Table IV show that our uncalibration reconstruction is valid. The rectangular vertex coordinates on the stripe planes were extracted manually here. This is due to the limited number of black and white rectangular grids used in this experiment. In practice, the projected patterns can be encoded, for example, by a certain color array [14], [22], in which case, the correspondences can be identified automatically.

Next, we used a workpiece to verify the uncalibrated 3-D reconstruction using our experimental vision system. The workpiece dimensions were measured by a caliper and are given in Fig. 9. The workpiece was placed at an arbitrary position and was illuminated by the pattern projection system. The pattern

TABLE VI
ANGULAR ERRORS IN UNCALIBRATION RECONSTRUCTION (UNIT: DEGREE)

	plane 1 and plane 2	plane 2 and plan3	plane 3 and plane4
Nominal angle	90.00	90.00	90.00
Recovered angle	90.268	90.281	89.920
Angle error	0.268	0.281	-0.08

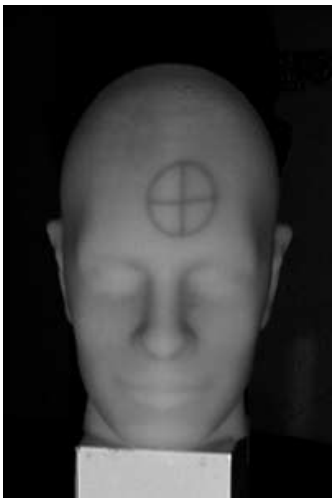

Fig. 12. Dummy head.

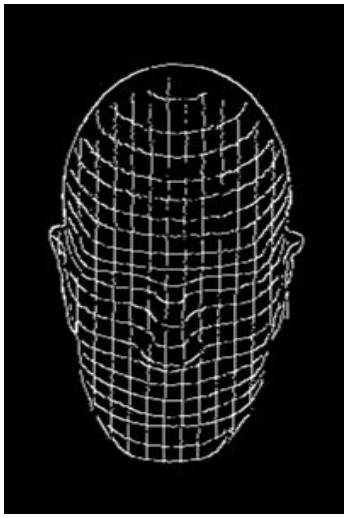

Fig. 13. Edge detection result from the pattern projected.

projector's parameters and its orientation relative to the world frame were precalibrated and were kept unchanged during this experiment. Thus, the stripe light plane's equations and their 2-D local coordinate systems with respect to the world frame were known during the reconstruction. We adjusted the cameras' intrinsic and extrinsic parameters to be able to capture the workpiece image illuminated by the projector, as shown in Fig. 10. No limits were imposed on the camera parameters. To reconstruct the 3-D surface of the workpiece, we need to recover the homographic matrices of the stripe light planes illuminating the object relative to the camera image planes. After the homographies were obtained, the object's 3-D surface were reconstructed, based on (23). The 3-D reconstruction result is shown in Fig. 11. Comparing the results with the real dimensions of the

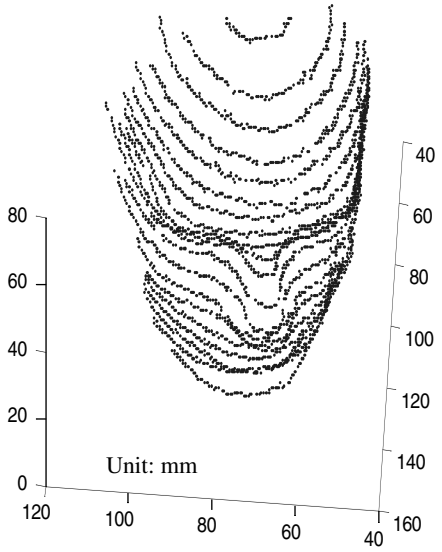

Fig. 14. Result of uncalibrated reconstruction.

workpiece given in Fig. 9, we obtained the reconstruction errors in distance between two planes, as given in Table V. The angular errors are given in Table VI. From the results, it is observed that the accuracy of the uncalibration reconstruction is quite high. In this experiment, the workpiece was placed at about 0.5 m from the baseline, defined as the line between the camera and projector's projective centers. The angle between the projector's projective axis and the baseline was around 45 degrees. In our experimental investigation of the sensitivity of the reconstruction, it was observed that the reconstruction accuracy could be affected by the distance from the object to the system/projector. In our tests, when the work piece was placed within the range of 0.4–0.8 m from the baseline, the maximum distance and angular errors in the reconstruction were found to be 0.11 mm and 0.47 degree, respectively. The increase in the errors is due mainly to the blurring effects in the projected stripe edges when the work piece is off from the best-focused location. This suggests a reference distance be used as an approximate standoff for an object to be measured by the system. As the reconstruction is also subject to the calibration errors of the projector [13], better results in the reconstruction can be expected if a more precise approach is taken in precalibrating the projector.

In yet another experiment, we conducted the uncalibrated reconstruction of a freeform surface, the face of a dummy head, as shown in Fig. 12, using the same experimental setup. Fig. 13 shows the preprocessed image. The horizontal curves and the vertical lines were extracted from the projected pattern by the Canny algorithm. As pointed out previously, only the horizontal curves contributed to the uncalibrated reconstruction. The vertical lines were merely used for recovering the homographies of the stripe planes. The reconstruction result is given in Fig. 14.

As can be seen, although the horizontal curves are quite sparse, so that the sampling points along the perpendicular direction are not dense, the reconstruction results turned out to be quite satisfactory.

VII. Conclusion

In this paper, we studied the issues in uncalibrated 3-D Euclidean reconstruction by active vision using pattern projections. The pattern projector is assumed to be precalibrated offline, whereas both the intrinsic and extrinsic parameters of the camera can be changed or even totally unknown in a reconstruction task. This allows the use of totally uncalibrated camera in the Euclidean reconstruction of the 3-D surface of a scene. The developed method was implemented with satisfactory experimental results. The system can work well for reconstructing free-form surfaces without requiring apparent features.

In traditional shape from motion, the camera's parameters are normally assumed to be constant, e.g., in 3-D reconstruction using a stereo head. Using our active vision system and the developed methodology, the 3-D Euclidean data of the scene can be obtained without any constraint on the parameters of the camera. Therefore, in our reconstruction, the camera parameters can be adjusted to suit the environment, giving the vision system the adaptability needed in many practical applications.

References

[1] S. J. Maybank and O. D. Faugeras, "A theory of self-calibration of a moving camera," *Int. J. Comput. Vis.*, vol. 8, no. 2, pp. 123–151, Nov. 1992.

[2] O. Faugeras, "What can be seen in three dimensions with an uncalibrated stereo rig? Computer vision—ECCV'92, lecture notes in computer science," in *Proc. 2nd European Conf. Computer Vision*, Santa Margherita Ligure, Italy, May 1992, pp. 563–578.

[3] R. I. Hartley, *Euclidean Reconstruction From Uncalibrated Views, Applications of Invariance in Computer Vision, Lecture Notes in Computer Science*. Berlin, Germany: Springer, 1993, vol. 852, pp. 237–256.

[4] O. Faugeras, "Stratification of three-dimensional vision: Projective, affine, and metric representations," *J. Opt. Soc. Amer. A*, vol. 12, no. 3, pp. 465–484, Mar. 1994.

[5] A. Fusiello, "Uncalibrated Euclidean reconstruction: A review," *Image Vis. Comput.*, vol. 18, no. 6–7, pp. 555–563, May 2000.

[6] M. Pollefeys, L. Van Gool, and M. Proesmans, "Euclidean 3-D reconstruction from image sequences with variable focal lengths," in *Proc. European Conf. Computer Vision*, vol. 1, Cambridge, U.K., 1996, pp. 31–42.

[7] Y. Seo and K. S. Hong, "About the self-calibration of a rotating and zooming camera: Theory and practice," in *Proc. 7th IEEE Int. Conf. Computer Vision*, vol. 1, Corfu, Greece, Sept. 1999, pp. 183–189.

[8] H. Kim and K. S. Hong, "A practical self-calibration method of rotating and zooming cameras," in *Proc. 15th Int. Conf. Pattern Recognition*, vol. 1, Barcelona, Spain, Sept. 2000, pp. 354–357.

[9] A. Heyden and K. Astrom, "Euclidean reconstruction from image sequences with varying and unknown focal length and principal point," in *Proc. IEEE Conf. Computer Vision and Pattern Recognition*, San Juan, PR, June 1997, pp. 438–443.

[10] M. Pollefeys, R. Koch, and L. V. Gool, "Self-calibration and metric reconstruction in spite of varying and unknown intrinsic camera parameters," *Int. J. Comput. Vis.*, vol. 32, no. 1, pp. 7–25, Aug. 1999.

[11] F. Kahl and A. Heyden, "Robust self-calibration and Euclidean reconstruction via affine approximation," in *Proc. 14th Int. Conf. Pattern Recognition*, vol. 1, Brisbane, Australia, Aug. 1998, pp. 56–58.

[12] Y. F. Li and Z. Liu, "Method for determining the probing points for efficient measurement and reconstruction of freeform surfaces," *Meas. Sci. Technol.*, vol. 14, no. 8, pp. 1280–1288, Aug. 2003.

[13] Y. F. Li and S. Chen, "Automatic recalibration of an active structured light vision system," *IEEE Trans. Robot. Automat.*, vol. 19, pp. 259–268, Apr. 2003.

[14] S. Chen and Y. F. Li, "Dynamically reconfigurable visual sensing for 3-D perception," in *Proc. IEEE Int. Conf. Robotics and Automation*, Taipei, Taiwan, Sept. 2003, pp. 2129–2134.

[15] D. Fofi, E. M. Mouaddib, and J. Salvi, "How to self-calibrate a structured light sensor," in *Proc. 9th Int. Symp. Intelligent Robotic System*, Toulouse, France, July 2001.

[16] D. Q. Huynh, R. A. Owens, and P. E. Hartmann, "Calibrating a structured light stripe system: A novel approach," *Int. J. Comput. Vis.*, vol. 33, no. 1, pp. 73–86, Sept. 1999.

[17] R. Hartley and A. Zisserman, *Multiple View Geometry in Computer Vision*. Cambridge, U.K.: Cambridge Univ. Press, 2000.

[18] G. Q. Wei and S. D. Ma, "Implicit and explicit camera calibration: Theory and experiments," *IEEE Trans. Pattern Anal. Machine Intell.*, vol. 16, pp. 469–480, May 1994.

[19] J. G. Semple and G. T. Kneebone, *Algebraic Projective Geometry*. New York: Oxford Univ. Press, 1998.

[20] L. Kadison and M. T. Kromann, *Projective Geometry and Modern Algebra*. Boston, MA: Birkhauser, 1996.

[21] C. H. Chen and A. C. Kak, "Modeling and calibration of a structured light scanner for 3-D robot vision," in *Proc. IEEE Int. Conf. Robotics and Automation*, Raleigh, NC, Mar. 1987, pp. 807–815.

[22] R. A. Morano *et al.*, "Structured light using pseudorandom codes," *IEEE Trans. Pattern Anal. Machine Intell.*, vol. 20, pp. 322–327, Mar. 1998.

Y. F. Li (M'91–SM'01) received the Ph.D. degree in robotics from the University of Oxford, Oxford, U.K. in 1993.

From 1993 to 1995, he was a Postdoctoral Research Associate in the AI and Robotics Research Group, Department of Computer Science, University of Wales, Aberystwyth, U.K. He joined City University of Hong Kong, Hong Kong in 1995, where he is currently an Associate Professor in the Department of Manufacturing Engineering and Engineering Management. His research interests include robot vision, 3-D vision, sensing, and sensor-based control for robotics.

R. S. Lu received the M.Sc. degree in 1995 and the Ph.D. degree in 1998 in precision instrument engineering, both from Hefei University of Technology, Hefei, China.

He then joined the Key Laboratory Precision Measuring Technology and Instrument in Tianjin University, Tianjin, China, as a Postdoctoral Researcher and later an Associate Professor, to perform research on image processing and 3-D machine vision inspection. From March 2001 to May 2002, he was a Research Associate and then Senior Research Associate at City University of Hong Kong, Kowloon, working on robot vision. He then was a Professor and the Director of Opto-electronic Engineering Institute, Hefei University of Technology. Currently, he is an Academic Researcher at Imperial College, London, U.K., on surface characteristic inspection. His research interests cover opto-electronics, machine vision, and digital image processing.